PHYSICAL REVIEW D **90,** 044042 (2014)

# Stability of Reissner-Nordström black hole in de Sitter background under charged scalar perturbation

Zhiying Zhu,[1,2] Shao-Jun Zhang,[1] C. E. Pellicer,[3] Bin Wang,[1] and Elcio Abdalla[4]

[1]*Department of Physics and Astronomy, Shanghai Jiao Tong University, Shanghai 200240, China*
[2]*Department of Physics and Electronic Science, Changsha University of Science and Technology, Changsha, Hunan 410076, China*
[3]*Escola de Ciências e Tecnologia, Universidade Federal do Rio Grande do Norte, Caixa Postal 1524, 59072-970 Natal, Rio Grande do Norte, Brazil*
[4]*Instituto de Física, Universidade de São Paulo, CEP 05315-970 São Paulo, Brazil*

(Received 16 May 2014; published 15 August 2014; publisher error corrected 20 August 2014)

We find a new instability in the four-dimensional Reissner-Nordström–de Sitter black holes against charged scalar perturbations with vanishing angular momentum, $l = 0$. We show that such an instability is caused by superradiance. The instability does not occur for a larger angular index, as explicitly proved for $l = 1$. Our results are obtained from a numerical investigation of the time-domain profiles of the perturbations.

DOI: 10.1103/PhysRevD.90.044042 PACS numbers: 04.70.Bw, 04.30.Nk, 42.50.Nn

## I. INTRODUCTION

Perturbations around black holes have been intriguing objects of discussions for decades. One of the main reasons is their astrophysical interest. Real black holes always have interactions with the respective astrophysical environment through absorption or evaporation processes. Starting from analyses of the perturbations around black holes, we can inquire about their stability. If black holes are unstable under small perturbations, they will inevitably be destabilized and disappear or transform dynamically into another object; thus, they simply cannot exist in nature as it is originally defined. For the $(3 + 1)$-dimensional asymptotically flat black holes, such as Schwarzschild, Reissner-Nordström (RN), and Kerr black holes, the corresponding stability has been checked thoroughly against different kinds of perturbations including neutral scalar, electromagnetic, and gravitational perturbations, and they were found stable. Analyses of these perturbations and proofs of stability of $(3 + 1)$-dimensional Schwarzschild–de Sitter (dS), RN-dS, and Kerr-dS black holes have been reported. Recently, motivated by the discovery of the correspondence between physics in the anti–de Sitter (AdS) spacetime and conformal field theory (CFT) on its boundary (AdS/CFT), the perturbations around four-dimensional AdS black holes have been examined, and $(3 + 1)$-dimensional AdS black holes were found stable under neutral scalar, electromagnetic, and gravitational perturbations. It was concluded that all of the considered four-dimensional black holes tested for stability are stable, except the string theory generalization of Kerr-Newman black holes whose stabilities have not been tested due to the difficulty in decoupling the angular variables in their perturbation equations. For a review on this topic, see [1,2], and references therein.

The physics in higher dimensions is much richer. In contrast to the four-dimensional results, various instabilities have been found. In a wide class of $D \geq 4$ configurations, such as black strings and black branes, the Gregory-Laflamme instability against linear perturbations was disclosed [3,4]. For high-dimensional black holes in the Einstein-Gauss-Bonnet theory, it was found that instabilities occur at higher multipoles $l$, while the first few lowest multipoles are stable [5,6]. Recently, in the high-dimensional RN-dS black hole background, numerical investigations have uncovered the surprising result that the RN black holes in dS backgrounds are unstable for spacetime dimensions larger than six [7,8].

The dynamical perturbations of a black hole background can usually be described by a single wavelike equation, where a growing mode of the perturbation indicates the instability of the black hole. Besides such a procedure, there also exists a superradiant instability in the black hole spacetime. Considering the classical scattering problem for a perturbation field in a black hole background, we can have superradiance, a phenomenon where the reflected wave has larger amplitude than the incident wave. If the effective potential contains an extra local minimum out of the black hole in addition to the local maximum, the superradiance will get successively amplified in the valley of the local potential near the black hole, which will result in the superradiant instability destabilizing the black hole. Reviews of the superradiance stability can be found in Refs. [1,9]. Most investigations on the superradiant instability were concentrated on the rotating black holes. Recently, the discussions of the superradiant stability were extended to the charged black holes with charged scalar field perturbations [10,11]. It was found that the superradiant instability can happen more efficiently when one considers charged black holes and charged scalar fields [12–14]. It would be of great interest to extend the study of the superradiant stability to black holes in the real Universe, namely, the black hole in the dS backgrounds.

 

We will study small charged scalar field perturbations in the vicinity of a $(3+1)$-dimensional RN black hole in a de Sitter background by doing numerical calculations. The stability of such black holes under charged scalar perturbations has never been examined previously. In the AdS spacetime, it was observed that the $(3+1)$-dimensional RN-AdS black hole can become unstable due to the condensation of the charged scalar hair onto the black hole. and finally the AdS black hole can be destabilized under a small charged scalar field perturbation [15–17]. Does this observed instability occur only for the AdS black holes because of their special spacetime properties? Will the dynamical stability also happen in other four-dimensional black hole backgrounds? It is of great interest to test whether the $(3+1)$-dimensional RN-dS black hole can remain stable as other four-dimensional black holes under such charged scalar perturbing fields. This is the first motivation of the present paper. Besides, we would like to explore whether the stability against linearized dynamical perturbations relates to the superradiant stability due to the superradiant amplification of charged scalar waves.

The organization of the paper is as follows. In Sec. II, we review the $(3+1)$-dimensional RN-dS black hole background and give the radial wave equation for a charged scalar field perturbation. In Sec. III, we use the finite difference method to study the time-domain perturbation evolution of the charged scalar field and test the stability against such perturbations. In Sec. IV, we derive the superradiant condition for the four-dimensional RN-dS black hole under a charged scalar perturbation and examine the relation between the dynamic stability and the superradiant stability. Finally, we provide conclusions in Sec. IV. We use natural units with $G=\hbar=c=1$.

## II. METRIC, PERTURBATION FIELDS, AND EFFECTIVE POTENTIALS

We consider a charged massive scalar field perturbation in the RN-dS black hole background with the metric

$$ds^2=-f(r)dt^2+\frac{1}{f(r)}dr^2+r^2(d\theta^2+\sin^2\theta d\phi^2), \tag{1}$$

where

$$f(r)=1-\frac{2M}{r}+\frac{Q^2}{r^2}-\frac{\Lambda r^2}{3}. \tag{2}$$

The integration constants $M$ and $Q$ are the black hole mass and electric charge, respectively. $\Lambda$ is the positive cosmological constant.

The spacetime causal structure depends strongly on the zeros of $f(r)$. Depending on the parameters $M$, $Q$, and $\Lambda$, the function $f(r)$ can have one to three or even no real positive zeros (for a negative cosmological constant). For the RN-dS cases we are interested in, $f(r)$ has three real, positive roots $(r_c, r_+, r_-.)$ and a real and negative root $r_0=-(r_-+r_++r_c)$. The horizons $r_-$, $r_+$, and $r_c$ are denoted as black hole Cauchy, event, and cosmological horizons, respectively, which satisfy $r_-<r_+<r_c$.

The metric function $f(r)$ can be expressed as

$$f(r)=\frac{\Lambda}{3r^2}(r-r_+)(r_c-r)(r-r_-)(r-r_o). \tag{3}$$

Introducing the surface gravity $\kappa_i=\frac{1}{2}|df/dr|_{r=r_i}$ associated with the horizon $r=r_i$, we can write the inverse of the metric function

$$\frac{1}{f}=-\frac{1}{2\kappa_-(r-r_-)}+\frac{1}{2\kappa_+(r-r_+)}+\frac{1}{2\kappa_c(r_c-r)}+\frac{1}{2\kappa_o(r-r_o)}. \tag{4}$$

Thus we can obtain the analytic form of the tortoise coordinate by calculating $r_*=\int f^{-1}(r)dr$:

$$r_*=-\frac{1}{2\kappa_-}\ln\left(\frac{r}{r_-}-1\right)+\frac{1}{2\kappa_+}\ln\left(\frac{r}{r_+}-1\right)-\frac{1}{2\kappa_c}\ln\left(1-\frac{r}{r_c}\right)+\frac{1}{2\kappa_o}\ln\left(1-\frac{r}{r_o}\right). \tag{5}$$

It is easy to see that $r_*\to-\infty$ as $r\to r_+$ and $r_*\to\infty$ as $r\to r_c$.

Consider now a charged scalar perturbation field $\psi$ obeying the Klein-Gordon equation

$$[(\nabla^\nu-iqA^\nu)(\nabla_\nu-iqA_\nu)-\mu^2]\psi=0, \tag{6}$$

where $q$ and $\mu$ are, respectively, the charge and mass of the perturbing field and $A_\mu=-\delta^0_\mu Q/r$ denotes the electromagnetic potential of the black hole. By adopting the usual separation of variables in terms of a radial field and a spherical harmonic $\psi_{lm}(t,r,\theta,\phi)=\Sigma_{lm}\frac{1}{r}\Psi_{lm}(t,r)\times S_{lm}(\theta)e^{im\phi}$, the Schrödinger-type equations in the tortoise coordinate for each value of $l$ read

$$-\frac{\partial^2\Psi}{\partial t^2}+\frac{\partial^2\Psi}{\partial r_*^2}+2iq\Phi\frac{\partial\Psi}{\partial t}-V(r)\Psi=0, \tag{7}$$

where $\Phi=-Q/r$ and the effective potential $V$ is given by

$$V(r)=-q^2\Phi^2(r)+f(r)\left(\frac{l(l+1)}{r^2}+\mu^2+\frac{f'(r)}{r}\right). \tag{8}$$

For a neutral massless scalar field perturbation, the effective potentials were described in Refs. [18–20], which vanish at the black hole and cosmological event horizons. However, for the charged scalar field perturbation, it is easy to see that, at both the black hole and cosmological event

horizons, the effective potentials are negative. It is believed that the effective potential $V$ describes the scattering of $\psi$ by the background curvature [21]. Usually, if the effective potential is negative in some region, growing perturbation can appear in the spectrum, indicating an instability of the system under such perturbations. However, in Ref. [22], it was argued that this is not always true. They found that some potentials with a negative gap still do not imply instability. The criterion to determine whether a system is stable or not against linear perturbation is whether the time-domain profile for the evolution of the perturbation is decaying or not, or, in more general terms, the potential has to permit the existence of bound states [23]. Thus, in order to study the stability of the RN-dS black hole against charged scalar perturbation, we have to examine the evolution of the perturbation. In calculating the wave equation to obtain the evolution of the perturbation, usually the quasinormal boundary conditions should be employed by defining the solution with the purely ingoing wave at the black hole event horizon and outgoing wave at the cosmological horizon.

## III. STABILITY ANALYSIS

We do not have analytic solutions to the time-dependent wave equation with the effective potentials considered here. We thus discretize the wave equation (7). Because of the appearance of the term $2iq\Phi\frac{\partial\Psi}{\partial t}$, the procedure used in Ref. [24] is not convenient here. One simple efficient discretization, used for example in Ref. [16], is to define $\Psi(r_*,t)=\Psi(j\Delta r_*,i\Delta t)=\Psi_{j,i}$, $V(r(r_*))=V(j\Delta r_*)=V_j$, and $\Phi(r(r_*))=\Phi(j\Delta r_*)=\Phi_j$ and to write (7) as

$$-\frac{(\Psi_{j,i+1}-2\Psi_{j,i}+\Psi_{j,i-1})}{\Delta t^2}+2iq\Phi_j\frac{(\Psi_{j,i+1}-\Psi_{j,i-1})}{2\Delta t}+\frac{(\Psi_{j+1,i}-2\Psi_{j,i}+\Psi_{j-1,i})}{\Delta r_*^2}-V_j\Psi_{j,i}+O(\Delta t^2)+O(\Delta r_*^2)=0. \tag{9}$$

With the initial Gaussian distribution $\Psi(r_*,t=0)=\exp[-\frac{(r_*-a)^2}{2b^2}]$ and $\Psi(r_*,t<0)=0$, we can derive the evolution of $\Psi$ by

$$\Psi_{j,i+1}=-\frac{(1+iq\Phi_j\Delta t)\Psi_{j,i-1}}{1-iq\Phi_j\Delta t}+\frac{\Delta t^2}{\Delta r_*^2}\frac{\Psi_{j+1,i}+\Psi_{j-1,i}}{1-iq\Phi_j\Delta t}+\left(2-2\frac{\Delta t^2}{\Delta r_*^2}-\Delta t^2V_j\right)\frac{\Psi_{j,i}}{1-iq\Phi_j\Delta t}. \tag{10}$$

In the following, we choose the parameters $a=10$ and $b=3$ in the Gaussian profile. Since the von Neumann stability conditions usually require that $\frac{\Delta t}{\Delta r_*}<1$, we use $\frac{\Delta t}{\Delta r_*}=0.5$ here. We will discuss the behavior of the field $\varphi=\Psi/r$ in the following.

It is necessary to point out that the time-domain profiles of perturbations include contributions from all modes. It was argued that this method is based on the scattering of the Gaussian wave on the potential barrier and is independent of the boundary conditions at the black hole event and cosmological horizons [25]. Therefore, it includes all possible instabilities due to different boundary conditions.

In order to extract dominant frequency from the time-domain profile of the perturbation, we will use the Prony method. We can fit the profile data by superposition of damping exponents [26]

$$\Psi(r,t)\simeq\sum_{i=1}^{p}C_ie^{-i\omega_i(t-t_0)}. \tag{11}$$

We consider a late time period, which starts at $t_0$ and ends at $t=N\Delta t+t_0$, where $N$ is an integer and $N\geq 2p-1$. Then Eq. (11) is valid for each value from the profile data:

$$x_n\equiv\Psi(r,n\Delta t+t_0)=\sum_{j=1}^{p}C_je^{-i\omega_jn\Delta t}=\sum_{j=1}^{p}C_jz_j^n. \tag{12}$$

The Prony method allows us to find $z_i$ in terms of the known $x_n$ and, since $\Delta t$ is also known, to calculate the quasinormal frequencies $\omega_i$.

### A. Neutral scalar perturbation

First, we use the finite difference method proposed in Ref. [16] to reexamine the neutral massless scalar field perturbations in RN-dS spacetime, which was first reported in Ref. [18] and later confirmed in Ref. [20]. For $l=0,1$ modes, we plot the potential in Fig. 1(a). We can see that for the $l=0$ mode there exists a negative potential well following a potential barrier near the cosmological event horizon. But for the $l=1$ mode the potential well does not exist. The time-domain evolution of the perturbation in Fig. 1(b) shows that, when $l=0$, the field rapidly settles down to a constant value after some quasinormal oscillations. When $l=1$, the perturbation field falls off exponentially after the quasinormal oscillations. These results show very good agreement with those observed in Refs. [18,20], which gives us confidence in the numerical method we employed. The neutral massless scalar field perturbations do not grow in the time-domain profiles, although there is a negative potential well when $l=0$. This shows that the RN-dS black hole is stable against the neutral massless scalar perturbation. But when the multipole index $l=0$, the late time tail of the neutral scalar perturbation settles down to a constant value, instead of a decay, implying that the $l=0$ mode is prone to instability.

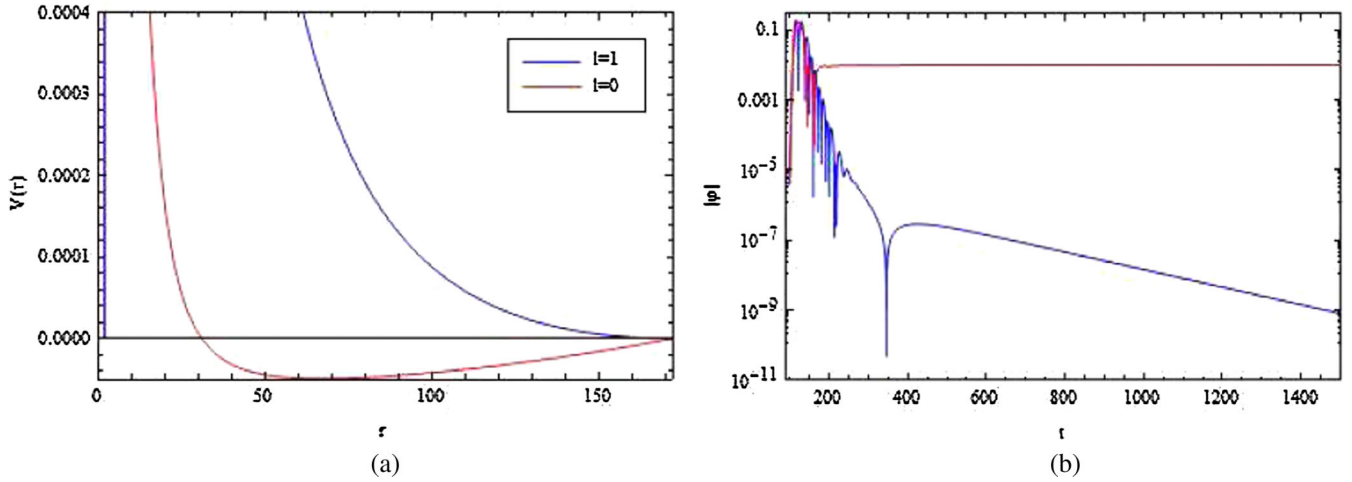


FIG. 1 (color online). (a) The potential and (b) the time-domain profiles of neutral massless scalar perturbations for $M = 1$, $Q = 0.5$, $\Lambda = 10^{-4}$, $l = 0$ (red line), and $l = 1$ (blue line). The potential $V(r)$ is obtained from the event horizon $r_+ = 1.866$ to the cosmological horizon $r_c = 172.197$. The field is shown outside the black hole at the position $r = 100$.

### B. Charged scalar perturbation

It is of great interest to extend the study to the charged scalar field perturbation. One expects that, with the new term in (9), the potential will become more negative when the scalar field is charged. Whether this can lead to a deeper potential well and destabilize the RN-dS black hole configuration is a question to be answered.

We first concentrate on the perturbation with the angular index $l = 0$ for the charged massless scalar field. In Fig. 2(a), we exhibit the potential behavior with the increase of the charge of the massless scalar field. It is clear that, with the increase of the charge of the scalar field, the potential has a wider and deeper negative well and the potential barrier becomes smaller. For a big enough charge $q$, i.e., $q \geq 2$, the potential barrier disappears and the potential falls continuously from a small negative value at the cosmological event horizon to a very negative constant at the black hole event horizon. Our main concern are regions where the effective potentials contain negative values, since possible instabilities are usually indicated in such regions.

The response of a stable RN-dS black holes to external charged scalar perturbation is determined by the late time evolution of the perturbation. In Fig. 2(b), we show the time-domain profiles for the evolution of charged scalar perturbations. When the scalar field is charged, the late time tail of the perturbation will grow in the end. With the increase of the charge of the scalar field, the growth will become stronger. This can be determined by the slopes of the late time tails. The growth of the charged scalar perturbation can be attributed to the negative potential well, which can trap and accumulate the perturbation and finally destabilize the background RN-dS black hole spacetime. But, when the charge of the scalar field is large

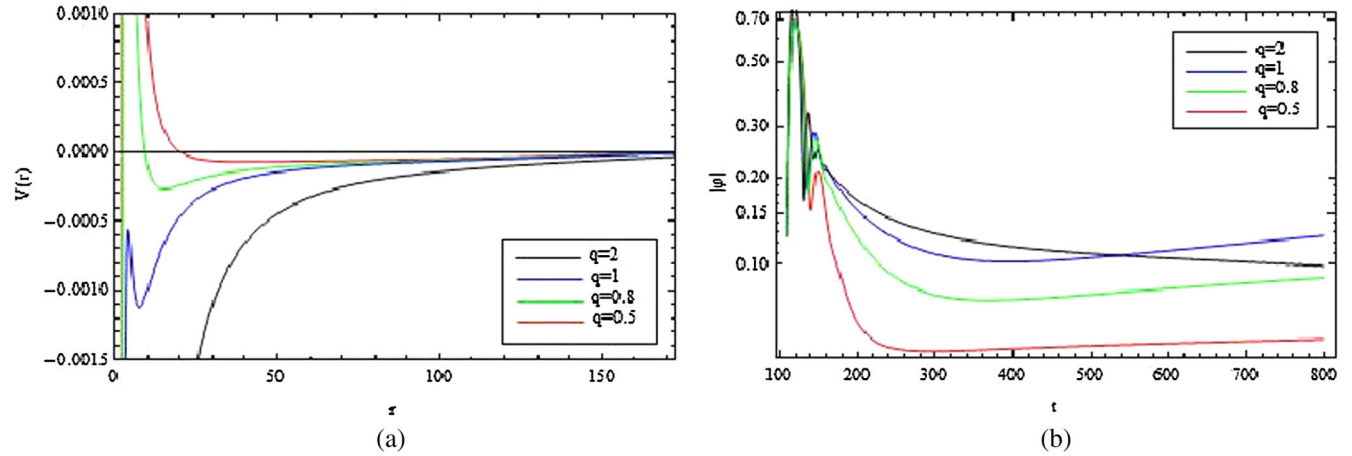


FIG. 2 (color online). (a) The potential and (b) the time-domain profiles of charged massless scalar perturbations for $M = 1$, $Q = 0.5$, $\Lambda = 10^{-4}$, $l = 0$, and $q = 0.5, 0.8, 1, 2$. The potential $V(r)$ is obtained from the event horizon $r_+ = 1.866$ to the cosmological horizon $r_c = 172.197$. The field is shown outside the black hole at the position $r = 100$.

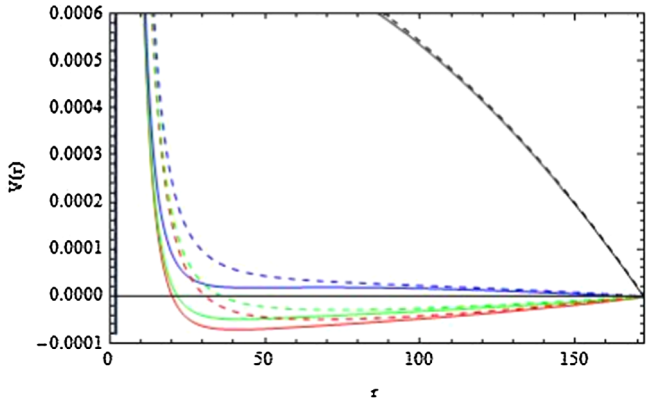


FIG. 3 (color online). The potential $V(r)$ is described from the event horizon $r_+ = 1.866$ to the cosmological horizon $r_c = 172.197$ with $M = 1$, $Q = 0.5$, $\Lambda = 10^{-4}$, and $l = 0$. The charge of the scalar field are $q = 0$ (dashed line) and $q = 0.5$ (solid line). The masses of the field are $\mu = 0$ (red line), $\mu = 0.005$ (green line), $\mu = 0.01$ (blue line), and $\mu = 0.03$ (black line) from bottom to top.

enough, its tail decays instead of growing in the end. This can be understood from the corresponding monotonic behavior in the potential, which cannot hinder the perturbation from falling into the black hole.

Above, we focused on the massless charged scalar field. It is of interest to explore the influence of the scalar field mass on the stability of the black hole. For the massive charged scalar field, we observe the influence on the potential by different values of the mass of the scalar field in Fig. 3. The dashed lines are for the neutral massive scalar fields, while the solid lines are for the charged scalar fields with different masses. We see that, when the scalar fields become more massive, the potential wells become narrower and less negative. When the mass of the scalar field is large enough, the potential will have only a positive barrier between the black hole and cosmological event horizons.

The evolution of perturbations is shown in Fig. 4. The dashed lines are for the neutral scalar field. We see that only

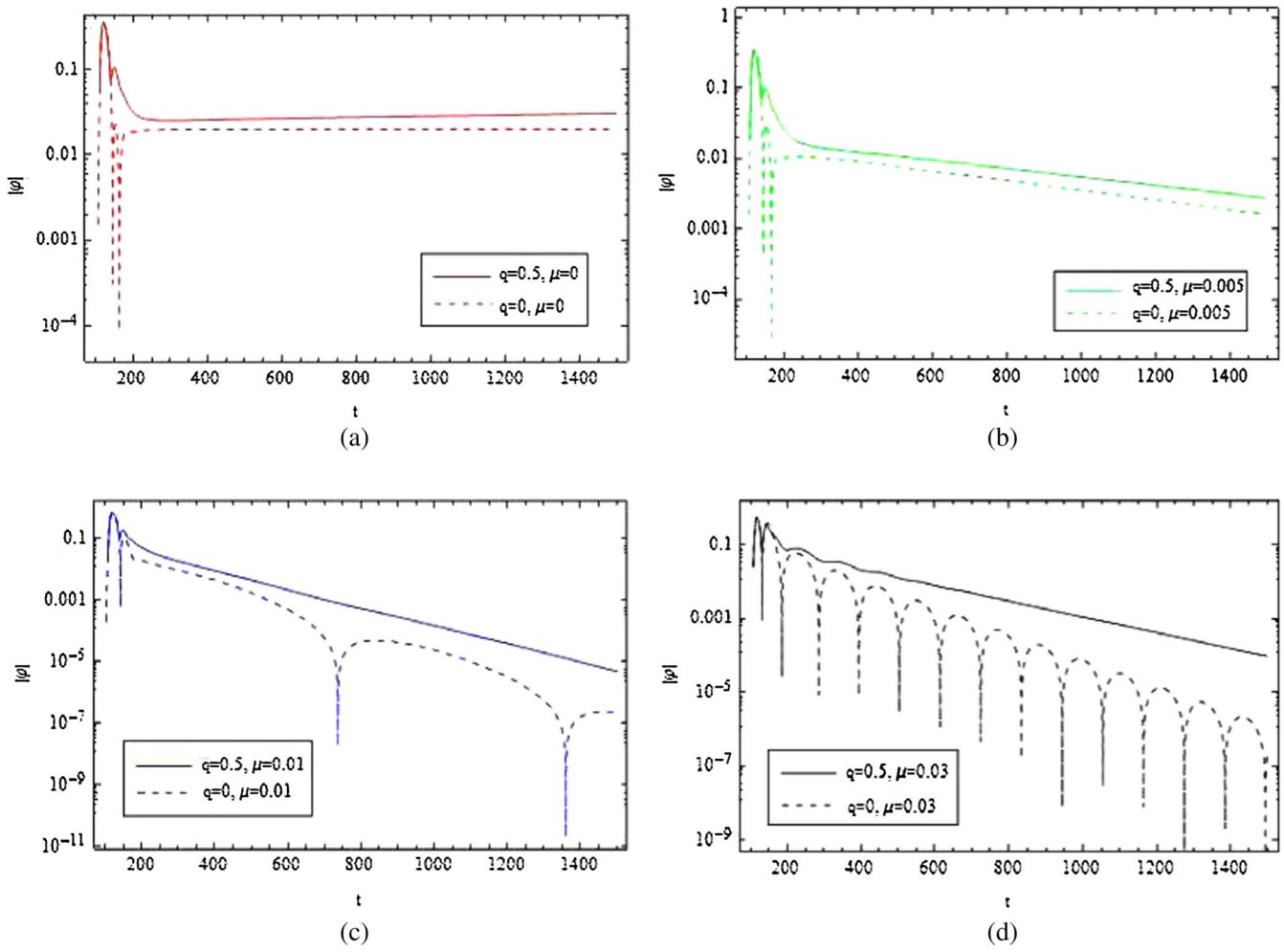


FIG. 4 (color online). Time-domain profiles for the scalar perturbations at $r = 100$ with $M = 1$, $Q = 0.5$, $\Lambda = 10^{-4}$, and $l = 0$. The solid lines and the dashed lines denote $q = 0.5$ and $q = 0$, respectively. The masses of the field are (a) $\mu = 0$, (b) $\mu = 0.005$, (c) $\mu = 0.01$, and (d) $\mu = 0.03$.

TABLE I. The decay rate of the scalar perturbations fit $\propto e^{\kappa t}$ at late time for $l = 0$, $M = 1$, $Q = 0.5$, and $\Lambda = 10^{-4}$. Here we obtained the value of $\kappa$ for different values of the charge and mass of the field.

| | $\mu = 0$ | $\mu = 0.0005$ | $\mu = 0.01$ | $\mu = 0.03$ |
|---|---|---|---|---|
| $q = 0$ | 0 | −0.00158 | −0.009 | −0.0083 |
| $q = 0.5$ | 0.000153 | −0.0014 | −0.0067 | −0.0049 |

for the massless scalar perturbation, which contains a constant tail, all massive perturbations exhibit a decay behavior at late time. When the mass of the scalar field is large enough, i.e., $\mu \geq 0.01$, neutral scalar perturbations have a long-lived ringing at the late time. The solid lines are for the scalar fields with fixed charge $q = 0.5$ but different masses. For the massless case, it exhibits a growing mode, but when the scalar field becomes massive, the perturbation decays. Fitting the curves in Fig. 4 with function $|\varphi| \propto e^{\kappa t}$ at late time, we can get the decay rate of perturbations in Table I. It is shown that, for both the neutral and charged scalar field perturbations, the decay of tails first becomes quicker and then slows down with the increase of the mass of the scalar field. The massive field exhibiting oscillations in the late time tail has higher energy, so that it decays slower. The influence of the scalar mass on the behavior of decay in the late time tail is consistent with that reported in the Kerr-Newman background [25].

In summary, we find that for the $l = 0$ mode, when the scalar field is charged, the perturbation can grow. But such growth can be avoided if we increase the mass of the scalar field. The RN-dS black hole background can be destabilized by the charged scalar field perturbation.

Now, we discuss the $l = 1$ perturbation mode. We first look at the massless but charged scalar field. In Fig. 5(a), we plotted the potential with the change of the charge $q$. It is similar to the one we observed for the $l = 0$ mode. With the increase of the charge, the region of negative potential becomes wider and deeper, while the potential barrier becomes lower. When the charge of the field is over a certain critical value, the potential becomes negative everywhere and decreases monotonically from the cosmological horizon to the black hole event horizon.

In contrast to the situation in the $l = 0$ mode, the potentials with negative wells here do not imply instability. The time-domain profiles of perturbation are shown in Fig. 5(b). We see that, when the charge of the scalar field increases, the decay of the perturbation tails becomes slower. We calculated that even until $q = 5$, which is 10 times the charge of the black hole itself, we still have the decay behavior of the perturbation. For larger $q$, in the numerical computation we require smaller $\Delta r_*$ to ensure convergence, what takes a much longer computation time. Thus, in contrast with the $l = 0$ case, the RN-dS black hole background remains stable against charged scalar perturbations when the angular index is $l = 1$. This result supports the argument given in Ref. [22], that the negative effective potential does not guarantee any growing mode in the time-domain profiles for the evolution of the perturbations. The negative potential well can be viewed as a necessary condition for the instability of the black hole, rather than a sufficient condition. Generally, a bound state structure is required for the equivalent Schrödinger problem [23].

For the $l = 1$ mode, the influence of the mass of the scalar field on the perturbation is illustrated in Fig. 6 for both neutral and charged scalar fields with fixed $q = 0.5$. It is shown that with the increase of the mass of the scalar field, no matter whether it is neutral or charged, the decay of perturbations first becomes quicker and then slows down. This result can be seen in Table II with the decay rate of perturbations fitted by $|\varphi| \propto e^{\kappa t}$ at late time and is

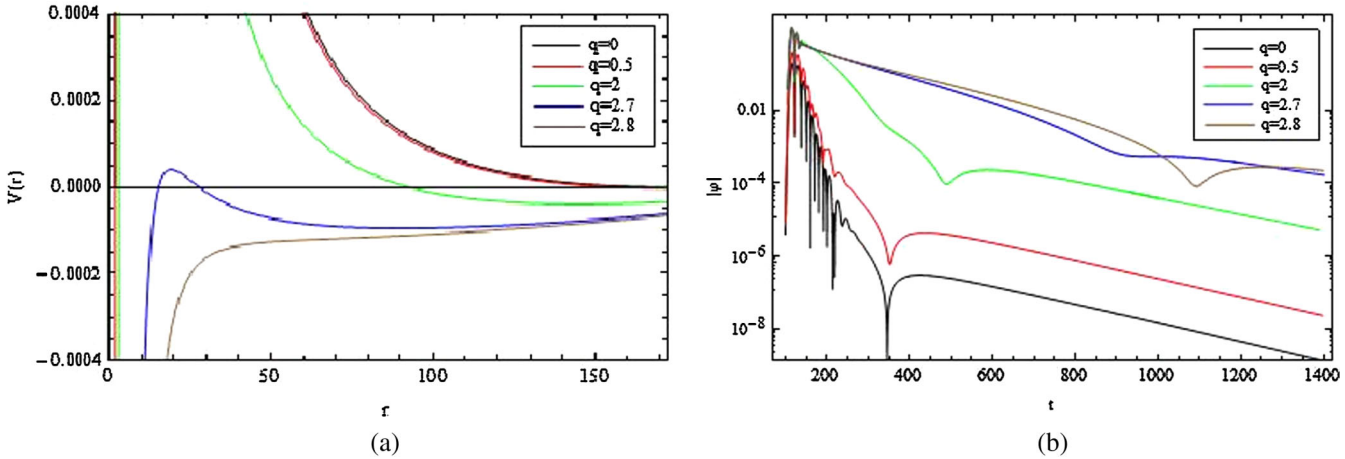


FIG. 5 (color online). (a) The potential and (b) the time-domain profiles of charged massless scalar perturbations for $M = 1$, $Q = 0.5$, $\Lambda = 10^{-4}$, $l = 1$, and $q = 0, 0.5, 2, 2.7, 2.8$. The potential $V(r)$ is obtained from the event horizon $r_+ = 1.866$ to the cosmological horizon $r_c = 172.197$. The field is shown outside the black hole at the position $r = 100$.

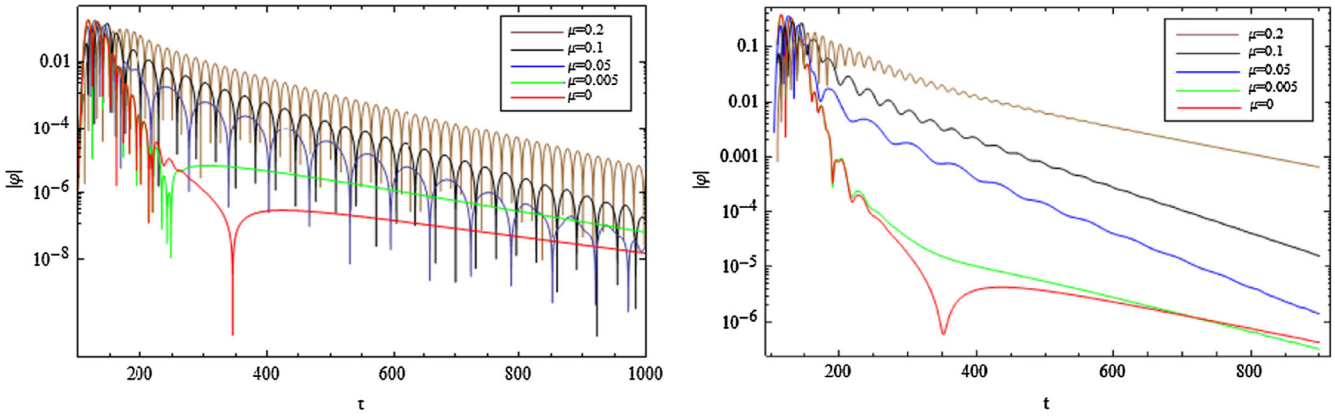


FIG. 6 (color online). Time-domain profiles for the scalar perturbations at $r = 100$ with $M = 1$, $Q = 0.5$, $\Lambda = 10^{-4}$, and $l = 1$. We consider (a) a neutral field and (b) a charged field with $q = 0.5$. The masses of the field are $\mu = 0$ (red line), $\mu = 0.005$ (green line), $\mu = 0.05$ (blue line), $\mu = 0.1$ (black line), and $\mu = 0.2$ (brown line).

consistent with the $l = 0$ case. When the mass of the scalar field is large enough, say, $\mu \geq 0.05$, one can see that the late time tail of a neutral scalar perturbation is dominated by a long-lived ringing. But for the charged scalar field, the ringing will be followed by an exponential tail.

## IV. DISCUSSION

The discussions presented in the previous section are focused on numerical calculations but do not offer much physical insight. Could the instability of the charged scalar field perturbation for the $l = 0$ state be triggered by the superradiant instability? If we look at the effective potential, there is a valley following the barrier. This is similar to the characteristic potential to accommodate the superradiant instability discussed in Refs. [10,11,14]. If there is superradiance, in the valley of the potential the reflection from the potential barrier could be amplified and its energy could be accumulated continuously, which could lead to instability.

For the RN-dS case, to examine the superradiant instability, we have to consider the classical scattering problem for the charged scalar field. The problem can be reduced to the wavelike equation

$$\frac{d^2\Psi}{dr_*^2} + (\omega^2 - \bar{V}(r))\Psi = 0, \tag{13}$$

with the effective potential

$$\bar{V}(r) = \frac{2qQ\omega}{r} - \frac{q^2Q^2}{r^2} + f(r)\left(\frac{l(l+1)}{r^2} + \mu^2 + \frac{f'(r)}{r}\right). \tag{14}$$

The effective potential has the following asymptotic behavior: when $r \to r_+$, $\bar{V} \approx \frac{2qQ\omega}{r_+} - \frac{q^2Q^2}{r_+^2}$ and when $r \to r_c$, $\bar{V} \approx \frac{2qQ\omega}{r_c} - \frac{q^2Q^2}{r_c^2}$, respectively. In a scattering experiment, (13) has the following asymptotic behavior:

$$\Psi \sim Be^{-i(\omega - qQ/r_+)r_*}, \quad \text{as } r \to r_+(r_* \to -\infty), \tag{15}$$

$$\Psi \sim e^{-i(\omega - qQ/r_c)r_*} + Ae^{+i(\omega - qQ/r_c)r_*}, \quad \text{as } r \to r_c(r_* \to \infty), \tag{16}$$

where $A$ is called the amplitude of the reflected wave or the reflection coefficient and $B$ is the transmission coefficient. We adopted the boundary condition that the wave comes from the cosmological horizon, partially passes through the potential barrier, and falls inside the event horizon, while the rest reflects back to the cosmological horizon [27,28]. Using the constancy of the Wronskian, we can show that

$$1 - |A|^2 = \frac{\omega - qQ/r_+}{\omega - qQ/r_c}|B|^2. \tag{17}$$

TABLE II. The decay rate of the scalar perturbations fit $\propto e^{\kappa t}$ at late time for $l = 1$, $M = 1$, $Q = 0.5$, and $\Lambda = 10^{-4}$. Here we obtained the value of $\kappa$ for different values of the charge and mass of the field.

| | $\mu = 0$ | $\mu = 0.0005$ | $\mu = 0.05$ | $\mu = 0.1$ | $\mu = 0.2$ |
|---|---|---|---|---|---|
| $q = 0$ | −0.00577 | −0.00736 | −0.0135 | −0.0129 | −0.0105 |
| $q = 0.5$ | −0.00566 | −0.00724 | −0.0114 | −0.00956 | −0.00551 |

TABLE III. Dominant modes for $M = 1$, $Q = 0.5$, $\Lambda = 10^{-4}$, and $l = 0$.

| $q$ | $\omega$ | $qQ/r_c$ | $qQ/r_+$ |
|---|---|---|---|
| 0.5 | $0.001508 + 0.000153i$ | 0.001452 | 0.133958 |
| 0.8 | $0.002559 + 0.000392i$ | 0.002323 | 0.214333 |
| 1 | $0.003414 + 0.000557i$ | 0.002904 | 0.267916 |
| 2 | $0.007487 - 0.000331i$ | 0.005807 | 0.535831 |

The reflected wave has larger amplitude than the incident one when

$$\frac{qQ}{r_c} < \omega < \frac{qQ}{r_+}. \tag{18}$$

Such an amplification of the incident wave is called superradiance. When the cosmological constant $\Lambda$ approaches to zero, $r_c$ becomes infinite, and the superradiant condition Eq. (18) is equivalent to the one for the RN black hole in the presence of charged scalar perturbations, $0 < \omega < qQ/r_+$ [10,11,29]. Here, $\omega$ is the real oscillation frequency of the perturbation.

Using the Prony method to fit the data in Fig. 2(b) at late time, we can obtain the dominant frequencies of the modes in Table III for charged scalar perturbations and vanishing angular momentum, $l = 0$. One can see that both the growing modes and decay mode satisfy the superradiant condition (18). This means that the instability that we found is caused by the superradiance, but not all the superradiant modes are unstable. This supports the discussion in a recent work [30], where it was argued numerically and analytically that the superradiance is a necessary condition, instead of a sufficient condition, for the instability.

## V. CONCLUSION

In this paper, we have investigated the stability of the RN-dS black hole. In the four-dimensional spacetime, the RN-dS black hole was found to be stable against the neutral scalar field perturbation [18–20]. However, recently, it has been reported that, when the spacetime dimensionality is $D > 6$, the RN-dS black hole can become unstable if there are small gravitational perturbations of scalar type [7,8]. Here we found that, even in the four-dimensional spacetime, the instability of a RN-dS black hole can appear under the perturbation of charged scalar field when the angular index vanishes. But when the angular index is unit, the background four-dimensional RN-dS black hole remains stable. We have noticed that the negative effective potential is not the only criterion to decide the stability of the background configuration; the practical tool for testing stability in spacetime backgrounds is the numerical investigation of the time-domain profiles of the perturbations. This supported the argument in Ref. [22] and the necessity of a bound state in the equivalent Schrödinger problem [23]. We have further explored the physical nature about why the instability is triggered by the $l = 0$ mode in the four-dimensional RN-dS black hole. We found that this instability is caused by superradiance, but not all the superradiant modes are unstable.

## ACKNOWLEDGMENTS

This work was supported in part by the National Natural Science Foundation of China. Z. Z. was also supported by China Postdoctoral Science Foundation under Grants No. 2011M500764 and No. 2012T50414. E. A. and C. E. P. thank FAPESP and CNPq (Brazil) for support.

[1] R. A. Konoplya and A. Zhidenko, Rev. Mod. Phys. **83**, 793 (2011).
[2] B. Wang, Braz. J. Phys. **35**, 1029 (2005).
[3] R. Gregory and R. Laflamme, Phys. Rev. Lett. **70**, 2837 (1993).
[4] R. Gregory and R. Laflamme, Nucl. Phys. **B428**, 399 (1994).
[5] R. A. Konoplya and A. Zhidenko, Phys. Rev. D **77**, 104004 (2008).
[6] M. Beroiz, G. Dotti, and R. J. Gleiser, Phys. Rev. D **76**, 024012 (2007).
[7] R. A. Konoplya and A. Zhidenko, Phys. Rev. Lett. **103**, 161101 (2009).
[8] V. Cardoso, M. Lemos, and M. Marques, Phys. Rev. D **80**, 127502 (2009).
[9] V. Cardoso, Gen. Relativ. Gravit. **45**, 2079 (2013).
[10] S. Hod, Phys. Lett. B **713**, 505 (2012).
[11] S. Hod, Phys. Lett. B **718**, 1489 (2013).
[12] J. C. Degollado, C. A. R. Herdeiro, and H. F. Rúnarsson, Phys. Rev. D **88**, 063003 (2013).
[13] S. Hod, Phys. Rev. D **88**, 064055 (2013).
[14] S.-J. Zhang, B. Wang, and E. Abdalla, arXiv:1306.0932.
[15] X. He, B. Wang, R.-G. Cai, and C.-Y. Lin, Phys. Lett. B **688**, 230 (2010).
[16] E. Abdalla, C. E. Pellicer, J. de Oliveira, and A. B. Pavan, Phys. Rev. D **82**, 124033 (2010).
[17] Y. Liu and B. Wang, Phys. Rev. D **85**, 046011 (2012).
[18] P. R. Brady, C. M. Chambers, W. Krivan, and P. Laguna, Phys. Rev. D **55**, 7538 (1997).
[19] P. R. Brady, C. M. Chambers, W. G. Laarakkers, and E. Poisson, Phys. Rev. D **60**, 064003 (1999).
[20] C. Molina, D. Giugno, E. Abdalla, and A. Saa, Phys. Rev. D **69**, 104013 (2004).
[21] E. S. C. Ching, P. T. Leung, W. M. Suen, and K. Young, Phys. Rev. Lett. **74**, 4588 (1995).
[22] K. A. Bronnikov, R. A. Konoplya, and A. Zhidenko, Phys. Rev. D **86**, 024028 (2012).
[23] A. Bachelot and A. Motet-Bachelot, Ann. I. H. P.: Phys. Theor. **59**, 3 (1993).
[24] B. Wang, C.-Y. Lin, and C. Molina, Phys. Rev. D **70**, 064025 (2004).

[25] R. A. Konoplya and A. Zhidenko, Phys. Rev. D **88**, 024054 (2013).
[26] E. Berti, V. Cardoso, J. A. González, and U. Sperhake, Phys. Rev. D **75**, 124017 (2007).
[27] U. Khanal, Phys. Rev. D **32**, 879 (1985).
[28] T. Tachizawa and K. Maeda, Phys. Lett. A **172**, 325 (1993).
[29] J. D. Bekenstein, Phys. Rev. D **7**, 949 (1973).
[30] R. A. Konoplya and A. Zhidenko, arXiv:1406.0019.